ELSEVIER

Journal of Alloys and Compounds 434–435 (2007) 327–332

Journal of ALLOYS AND COMPOUNDS

www.elsevier.com/locate/jallcom

Bulk amorphous alloy $Fe_{72}Al_5Ga_2C_6B_4P_{10}Si_1$ produced by mechanical alloying

T.R. Chueva [a], N.P. Dyakonova [b], V.V. Molokanov [a], T.A. Sviridova [b,*]

[a] *Institute of Metallurgy and Materials Science, Russian Academy of Sciences, Leninsky Pr. 49, Moscow 117911, Russia*
[b] *Moscow State Institute of Steel and Alloys, Technological University, Leninsky Pr. 4, Moscow 117936, Russia*

Available online 17 October 2006

Abstract

Mechanochemical synthesis of amorphous $Fe_{72}Al_5Ga_2C_6B_4P_{10}Si_1$ alloy starting from different initial ingredients (pre-alloys mixture Fe–Al–Ga–P, Fe–C–B–Si and previously melted ingot of the aimed composition) was investigated by X-ray diffraction and thermal analysis. Comparison between the resulting amorphous powders and rapidly quenched (RQ) amorphous ribbon of the same composition as regards the thermal stability, diffraction halo width and crystallization products was carried out. Complete amorphization was achieved only if pre-alloys mixture was used as initial ingredients. On thermal stability this amorphous phase is practically identical to amorphous RQ ribbon and has sufficiently wide range between the temperatures of glass-transition and crystallization.

Keywords: Amorphous materials; Amorphisation; High-energy ball milling; X-ray diffraction; Thermal analysis

1. Introduction

Multicomponent bulk metallic glasses are a new class of materials in which the amorphous state in centimetre-sized volumes is obtained by conventional metallurgical methods [1–3]. However for Fe-based bulk metallic glasses of large practical importance the thickness of amorphous layer does not exceed millimetres [4,5]. That is why the mechanochemical synthesis (MS) is a promising technology for such alloys which allows to obtain bulk products of any thickness and shape as a result of amorphous powder compacting in the temperature range from glass-transition temperature (T_g) to crystallization one (T_x) where the viscous flow of a material occurs [6–8].

In this work the possibility to obtain the well-known soft-magnetic alloy $Fe_{72}Al_5Ga_2C_6B_4P_{10}Si_1$ [9–11] in amorphous state by MS method has been studied. However, this alloy is hard to produce by mechanical alloying of pure elements because their mechanical properties significantly differ [12]. Therefore the amorphous powder of the alloy has been produced either by mechanical milling of crystalline ingot of target composition or by MS of Fe–Al–Ga–P and Fe–C–B–Si pre-alloys mixture.

2. Experimental details

The high-energy planetary ball mill of AGO-2U type with plate rotational frequency 685 rpm was used for MS. Two milling modes with ball-to-powder ratio 10:1 and 20:1 were applied, whereas the total ball mass 200 g was kept constant. These two modes correspond to energy intensities (E) 6.3 and 12.6 W/g, respectively [13]. Argon atmosphere was used for MS and sampling during milling. The milling time varied from 15 min to 12 h.

X-ray diffraction (XRD) patterns were taken with Co Kα-radiation using step scanning DRON-4 diffractometer. While analyzing the samples with amorphous phase (AP) a modification of Rietveld full profile fitting method [14] was employed with addition of experimental X-ray pattern of the pure AP reference (RQ ribbon) rescaled into theoretical units of intensity [13].

Thermal stability and crystallization of AP on heating was investigated by differential thermal analysis (DTA-7 HT thermal analyzer) in He atmosphere. Heating rate was 100 K/min.

3. Results

The alloy target composition was to be obtained by interfusion of two pre-alloyes $Fe_{66}Al_{10}Ga_4P_{20}$ and $Fe_{78}C_{12}B_8Si_2$ which were the initial ingredients on mechanical milling. The pre-alloys were chosen so as to be glass forming [15,16] or easily amorphized compounds (of Ti_3P and Fe_3C structure types, respectively). However, both pre-alloys in initial state proved to be constituted of two phases. The pre-alloy $Fe_{66}Al_{10}Ga_4P_{20}$ consisted of α-Fe solid solution with lattice parameter $a = 0.2904$ nm and phase $(Fe,Al,Ga)_2P$ of structure

* Corresponding author.
E-mail address: tim-17@yandex.ru (T.A. Sviridova).

0925-8388/$ – see front matter © 2006 Elsevier B.V. All rights reserved.
doi:10.1016/j.jallcom.2006.08.308

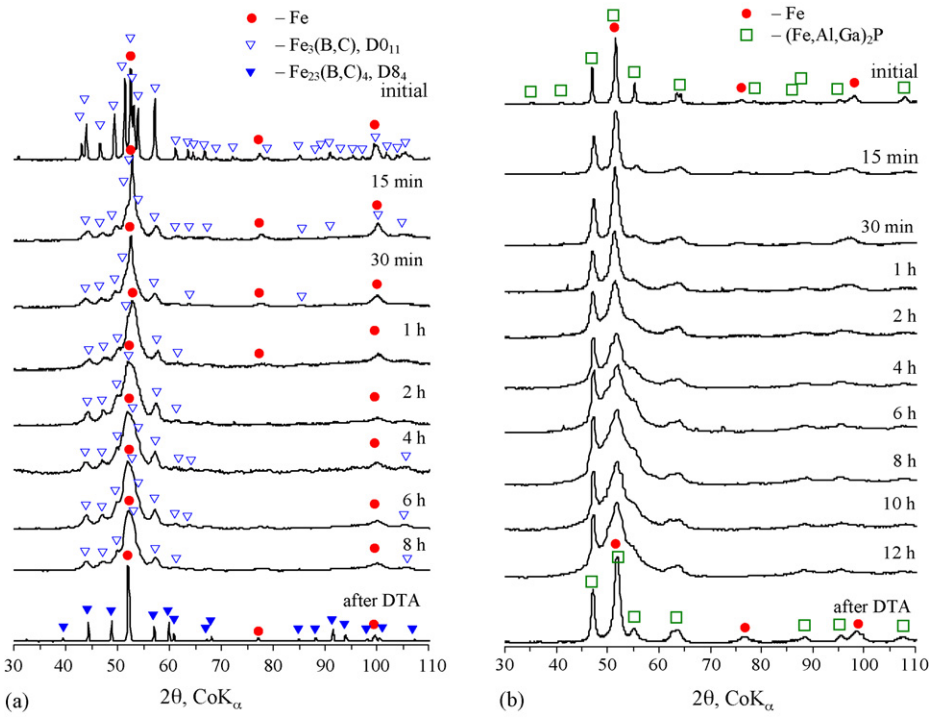

Fig. 1. X-ray diffraction patterns of pre-alloys: (a) $Fe_{78}C_{12}B_8Si_2$ and (b) $Fe_{66}Al_{10}Ga_4P_{20}$ after different milling time followed by DTA annealing.

type Fe_2P. The pre-alloy $Fe_{78}C_{12}B_8Si_2$ besides α-Fe solid solution with lattice parameter $a = 2.859$ Å contained a phase with cementite crystal structure $Fe_3(C,B)$.

Amorphisation of each pre-alloy on mechanical milling was investigated prior to MS of their mixture. The pre-alloys XRD patterns after processing in the ball mill are presented in Fig. 1. The milling led to peak broadening of crystalline phases. On milling the pre-alloy $Fe_{66}Al_{10}Ga_4P_{20}$ for 2 h, a diffuse halo arose that indicated a large volume fraction of AP in the sample. However the complete amorphization of this pre-alloy did not occur even after 12 h of milling. As regards pre-alloy $Fe_{78}C_{12}B_8Si_2$, even partial amorphization wasn't detected during any milling time.

DTA data (Fig. 2) agree with XRD results. There is a crystallization peak in DTA curve of pre-alloy $Fe_{66}Al_{10}Ga_4P_{20}$,

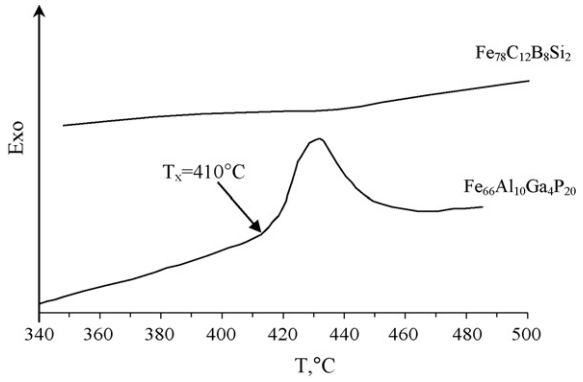

Fig. 2. DTA curves of $Fe_{66}Al_{10}Ga_4P_{20}$ and $Fe_{78}C_{12}B_8Si_2$ pre-alloys after most prolonged mechanical milling.

which confirms AP presence in the sample. Slight effects are observed in DTA curve of pre-alloy $Fe_{78}C_{12}B_8Si_2$ but neither of them relates to crystallization. After DTA the pre-alloy $Fe_{66}Al_{10}Ga_4P_{20}$ recovers initial phase composition whereas in pre-alloy $Fe_{78}C_{12}B_8Si_2$ the cubic carboboride $Fe_{23}(C,B)_6$ with crystal structure $Cr_{23}C_6$ and lattice parameter $a = 1.059$ nm replaces the phase with cementite crystal structure.

The MS of pre-alloys $Fe_{66}Al_{10}Ga_4P_{20}$ and $Fe_{78}C_{12}B_8Si_2$ mixture was carried out at two milling intensities. The diffraction patterns of samples after MS are shown in Fig. 3 which demonstrates that both regimes led to practically complete and quick transformation to amorphous state. Complete amorphization by MS with higher energy intensity occurred after 6 h of milling (Fig. 3a). The amorphization was also observed at low intensity regime (Fig. 3b), though this process proceeded slower. The comparison of Fig. 3a and b shows that about twice as much time is required to obtain the same phase distribution when operating at half power.

The ingot of alloy under consideration was also milled directly. The XRD patterns of milling products in relation to processing time are presented in Fig. 4. The ingot in initial state consisted of three phases: phase of structure type Fe_3P (type $D0_e$), phase Fe_3AlC_x (type $E2_1$) which is an fcc-based superstructure filled by metalloid and α-Fe solid solution with lattice parameter $a = 0.2880$ nm. During ingot milling the transformation of X-ray patterns to amorphous-like proceeded with higher rate though the traces of crystalline phases are detected even after 12 h of milling (Fig. 4).

The data for amorphization kinetics are presented in Fig. 5. At the initial stage of the process the transformation rate was substantially larger for the ingot, but despite that pure AP was

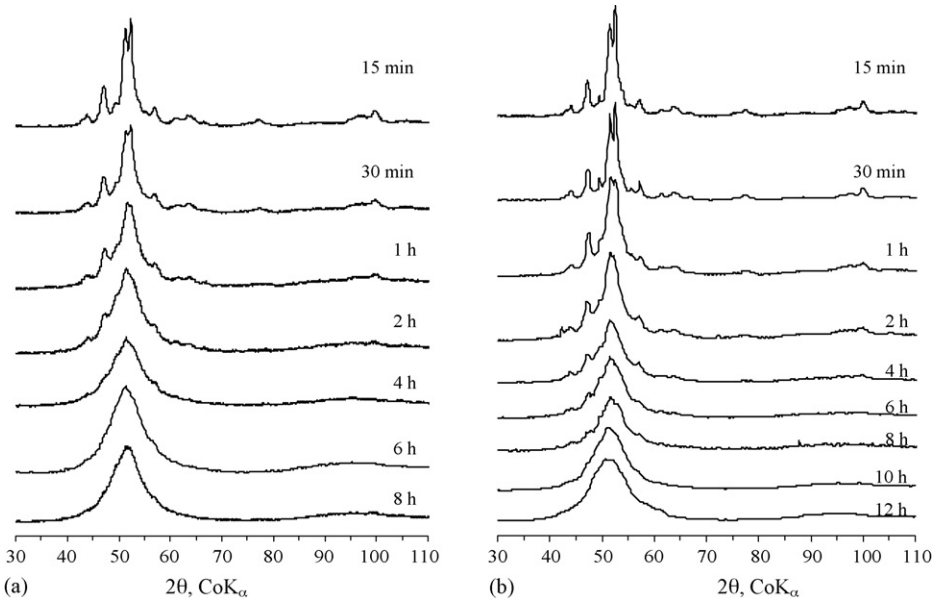

Fig. 3. X-ray patterns of pre-alloys mixture $Fe_{66}Al_{10}Ga_4P_{20}$ and $Fe_{78}C_{12}B_8Si_2$ depending on MS time with energy intensity: (a) $E = 12.6$ W/g; (b) $E = 6.3$ W/g.

attained only by MS of pre-alloys mixture with high-energy intensity level 12.6 W/g.

To compare the amorphous phases obtained by different methods the integral width of 1st diffuse halo maximum was measured. It is common knowledge that halo angular coordinate (center of gravity) depends on average interatomic distance $\langle d \rangle$ in AP, whereas its width is defined by dispersion of neighbouring interatomic distance. The multicomponent amorphous alloy should inevitably have the large dispersion $\langle d \rangle$ following from the different chemical (and due to size factor topological) surroundings of atoms. However, different amorphous states may exist within the same composition of alloy. The halo width depends on short-range order in AP and in some cases on the degree of chemical homogeneity. The halo width of amorphous phases are presented in Table 1 where data for amorphous reference (RQ ribbon) are also given.

Table 1
The integral width of the first diffuse halo maximum in XRD patterns of $Fe_{72}Al_5Ga_2C_6B_4P_{10}Si_1$ alloy produced by different methods

Preparation method	E (W/g)	Time (h)	Halo width, 2θ (°)
Rapid quenching	–	–	9.4
MS of pre-alloys mixture	12.6	4	11.9
$Fe_{66}Al_{10}Ga_4P_{20}$ and $Fe_{78}C_{12}B_8Si_2$	12.6	8	11.4
Mechanical milling of ingot	6.3	6	10.4
	6.3	12	12.4

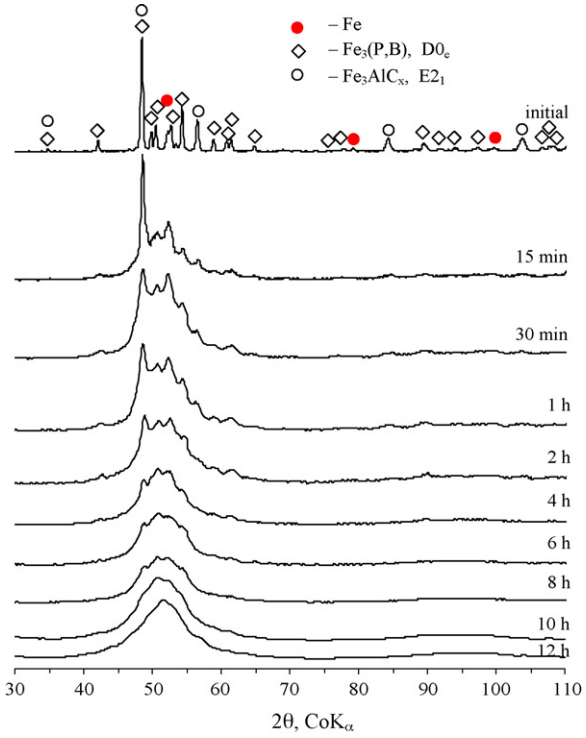

Fig. 4. X-ray patterns of $Fe_{72}Al_5Ga_2C_6B_4P_{10}Si_1$ alloy ingot after various milling times.

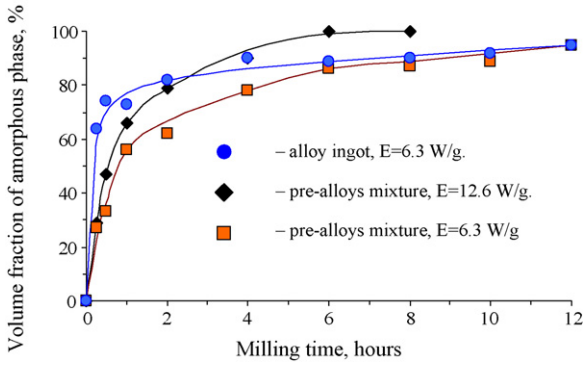

Fig. 5. Amorphization kinetics of $Fe_{72}Al_5Ga_2C_6B_4P_{10}Si_1$ alloy during processing by ball milling.

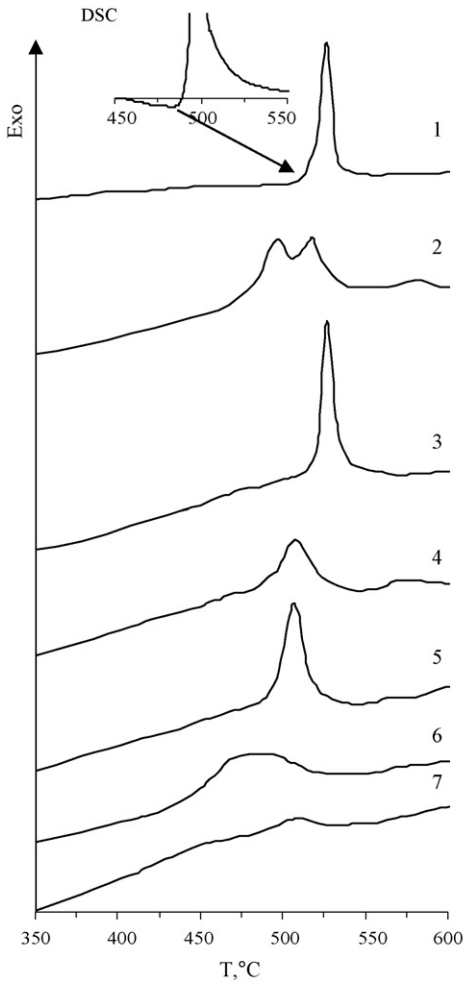

Fig. 6. Thermograms of $Fe_{72}Al_5Ga_2C_6B_4P_{10}Si_1$ alloy produced by different methods: rapid quenching (1); MS of pre-alloys mixture; (2) milled 4 h, $E = 12.6$ W/g; (3) milled 8 h, $E = 12.6$ W/g; (4) milled 6 h, $E = 6.3$ W/g; (5) milled 12 h, $E = 6.3$ W/g; (6) milled 6 h, $E = 6.3$ W/g; (7) milled 12 h, $E = 6.3$ W/g.

As it follows from the data presented in Table 1, the RQ amorphous ribbon had the narrowest halo and hence the most chemical homogeneity. On MS of pre-alloys mixture ($E = 12.6$ W/g) the halo width decreased in milling time range 4–8 h, whereas in the case of ingot the halo width increased with growth of processing time from 6 to 12 h.

All samples obtained by milling of various initial ingredients were subjected to thermal analysis and the results were compared with DTA-behaviour of RQ reference (Fig. 6). The transformation temperatures based on DTA curves are collected in Table 2.

The DTA data corroborate that amorphization of pre-alloys mixture by MS takes place. The transition to amorphous state under treatment with $E = 12.6$ W/g was accomplished after 8 h. It is evident from the similarity between DTA curves 3 (MS) and 1 (RQ) and therefore from close correspondence of temperatures T_g and T_x between sample and reference. There are two transitions in DTA-curve 2 after 4 h of MS, the crystallization temperature being about 30° lower than in amorphous reference. AP obtained by MS with less energy intensity (curve 5) has a lower crystallization temperature, T_g being absent in the curve. The width of transformation peak decreases as milling time grows (curves 4 and 5), approaching one of crystallization effect of the fully amorphous ribbon and powder (curves 1 and 3).

The DTA data on powders obtained by ingot milling revealed a broad peak with noticeably low transformation temperature $T_x = 426$ °C after treatment time 6 h (curve 6). After 12 h of processing 2 weak and smeared effects are observed in DTA curve 7. For the curves 6 and 7 DTA data contradicts X-ray analysis because the shape of DTA-curves is not typical for AP crystallization despite amorphous-like diffraction patterns of corresponding samples.

From the Table 2 it follows that amorphous alloy obtained by MS from pre-alloys mixture with $E = 12.6$ W/g and amorphous reference have practically the same T_x but slightly different $\Delta T = T_x - T_g$ range. Thus the thermal stability parameters of both amorphous phases are almost identical, however these amorphous phases differ in halo width.

Crystallization products of amorphous phases obtained by different methods were compared. These products are very close to each other as can be seen from Fig. 7. In all cases the compound of type Fe_3P ($D0_e$) and solid solution on the base of α-Fe formed after crystallization. Moreover the phase with cementite structure $Fe_3(C,B)$ (type $D0_{11}$) is present in all milled samples no matter what the initial ingredients were. Fcc-based superstructure (type $E2_1$) are present in all cases except the ingot.

4. Discussion

Mechanochemical synthesis of two pre-alloys led to AP formation and energy intensity affected only the time of transition to amorphous state. The AP obtained by MS is shows lower

Table 2
Milling treatment and thermal stability parameters of $Fe_{72}Al_5Ga_2C_6B_4P_{10}Si_1$ alloy produced by different methods

Preparation method	E (W/g)	Time (h)	T_g (°C)	T_{x1} (°C)	ΔT (°C)	T_{x2} (°C)	T_{x3} (°C)
Rapid quenching	–	–	453	511	58	–	–
MS of pre-alloys mixture $Fe_{66}Al_{10}Ga_4P_{20}$ and $Fe_{78}C_{12}B_8Si_2$	12.6	4	–	478	–	517[a]	557
	12.6	8	481	518	37	–	–
	6.3	6	–	480	–	–	550
	6.3	12	–	490	–	–	–
Mechanical milling of ingot	6.3	6	–	426	–	540	–
	6.3	12	–	414	–	485	–

[a] Peak position in DTA curve.

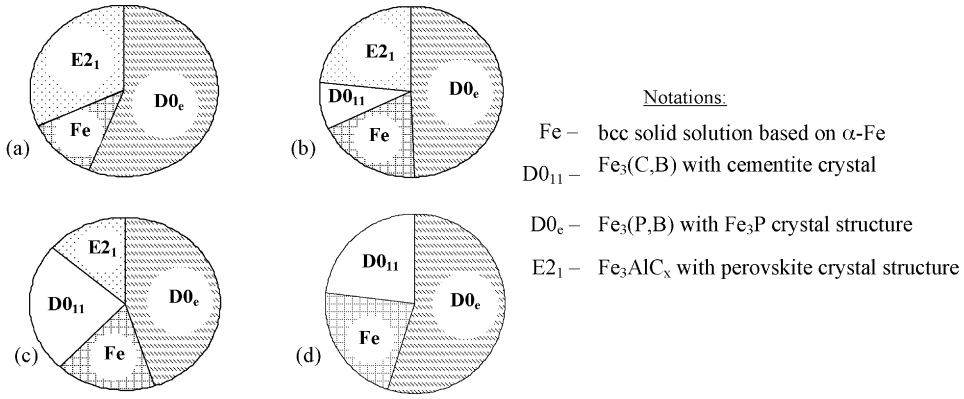

Fig. 7. Phase distribution in $Fe_{72}Al_5Ga_2C_6B_4P_{10}Si_1$ alloy produced by different methods after crystallization from amorphous state: (a) rapid quenching; (b) MS of pre-alloys mixture (E = 12.6 W/g, 8 h); (c) MS of pre-alloys mixture (E = 6.3 W/g, 12 h); (d) mechanical milling of ingot during 12 h.

halo width than the RQ ribbon but resembles it as regards T_g and rather wide $\Delta T = T_x - T_g$

The DTA-curve for intermediate milling time (curve 2, Fig. 6) indicates the possible amorphization mechanism. Such curve shape could be related to coexistence of two amorphous phases with different crystallization temperatures, in other words, chemical heterogeneity, which can be responsible for abnormal amorphous halo width. However if lesser energy intensity is applied the one-step crystallization occurred. (curve 4, Fig.6). Perhaps, in this case the crystallization proceeds in two stages as before but maxima of exothermic peaks are closely spaced. It can be noted that crystallization peak width in curves 4 and 5 (Fig. 6) decreases with milling time, as well as the halo width. This is evidence that AP heterogeneity decreases as milling time increases.

Two different amorphous phases probably differ in chemical composition. It is likely that each pre-alloy give rise to the related AP at the onset of transformation. As this takes place, it can be suggested that the presence of pre-alloy $Fe_{66}Al_{10}Ga_4P_{20}$, which is prone to partial amorphization, facilitates the conversion of more stable pre-alloy $Fe_{78}C_{12}B_8Si_2$ into amorphous state. The eutectic character of interaction between pre-alloys leads to complete amorphization of their mixture, i.e. the interphase surfaces may play a significant part in attaining pure amorphous state.

The analysis of crystallization products gives indirect evidence that powders include segregations with composition close to $Fe_{78}C_{12}B_8Si_2$: all annealed samples contain intermetallic compound with cementite structure in addition to the main phase constituent of Fe_3P type, whereas the cementite-like phase is not detected in the reference (RQ) after DTA heating.

According to XRD, in the course of ingot comminution attention, very fast amorphization occurs. However the presence of slight and smeared heat effects instead of sharp exothermic crystallization peak points to transformation into amorphous-like or ultrafine nanostructured state with nanometer-sized crystallites. Judging from phase content after DTA, milled ingot may consist of ultrafine mixture of phases $Fe_3(C,B)$, $Fe_3(P,B)$ and Fe-based solid solution. In [17] milling of the same alloy ingot led to the AP formation. The mill used in [17] had lower rotational frequency, therefore we suppose that in our case nanostructural state formation can be explained by annealing of AP *in situ* since the temperature of powder in the vial can reach 250–350 °C [13].

5. Conclusion

The possibility of obtaining alloy $Fe_{72}Al_5Ga_2C_6B_4P_{10}Si_1$ in amorphous state by mechanochemical synthesis from various ingredients (mixture of pre-alloys $Fe_{66}Al_{10}Ga_4P_{20}$ and $Fe_{78}C_{12}B_8Si_2$ or previously melted ingot) was studied and the resulting amorphous powders were compared with rapidly quenched ribbon as regards thermal stability, amorphous halo width and crystallization products.

The complete amorphization is feasible only if the pre-alloy mixture of $Fe_{66}Al_{10}Ga_4P_{20}$ and $Fe_{78}C_{12}B_8Si_2$ is used as initial ingredients. The amorphous phase obtained from mixture of pre-alloys with energy intensity 12.6 W/g and rapidly quenched amorphous ribbon have practically the same thermal stability and rather wide internal between the temperatures of glass-transition and crystallization. However these amorphous phases differ in amorphous halo width and crystallization products.

Acknowledgement

This work was partially supported by Russian Foundation for Basic Research RFBR (Grants No. 04-03-32700).

References

[1] A. Inoue, T. Zhang, T. Masumoto, Mater. Trans. JIM V 31 (1990) 425.
[2] A. Inoue, Acta Mater. 48 (2000) 279.
[3] A. Inoue, T. Zhang, A. Takeuchi, Mater. Sci. Forum 269–272 (1998) 855.
[4] A. Inoue, Acta Mater. 48 (2000) 279–306.
[5] A. Inoue, A. Makino, T. Mizushima, J. Magn. Magn. Mater. 215–216 (2000) 246–252.
[6] H. Kato, A. Kawamura, A. Inoue, Mater. Trans. JIM 37 (1996) 70.
[7] M. Siedel, J. Eckert, H.-D. Bauer, L. Schultz, Mater. Sci. Forum 225–227 (1996) 119.
[8] E.A. Zakharova, N.P. Dyakonova, T.A. Sviridova, M.I. Petrzhik, Materialovedenie 46–49 (11) (2001) (in Russia).
[9] A. Inoue, J.S. Gook, Mater. Trans. JIM 36 (1995) 1180.
[10] A. Inoue, J.S. Gook, Mater. Trans. JIM 36 (1995) 1282.

[11] N. Schlorke, J. Eckert, L. Schultz, J. Phys. D: Appl. Phys. 32 (1999) 855–861.
[12] D.R. Maurice, T.H. Courtney, Metall. Trans. A 21A (1990) 289–303.
[13] E.V. Shelekhov, T.A. Sviridova, Materialovedenie 10 (1999) 13–22.
[14] E.V. Shelekhov, T.A. Sviridova, Met. Sci. Heat Treatment 42 (7) (2000) 309–313.
[15] M.I. Petrzhik, V.V. Molokanov, R.A.N. Izv, Izv. RAN Ser. Phys. 65 (10) (2001) 1384–1389 (in Russia).
[16] N.P. Djakonova, T.A. Sviridova, E.A. Zakharova, V.V. Molokanov, M.I. Petrzhik, J. Alloys Compd. 367 (1–2) (2004) 191–198.
[17] N. Schlorke, J. Eckert, L. Schultz, J. Phys. D: Appl. Phys. 32 (1999) 855–861.